Finite size effects and 2-string deviations in the spin-1 XXZ chains

2007 J. Phys. A: Math. Theor. 40 12007

(http://iopscience.iop.org/1751-8121/40/40/001)

IOP Publishing Journal of Physics A: Mathematical and Theoretical

J. Phys. A: Math. Theor. **40** (2007) 12007–12032 doi:10.1088/1751-8113/40/40/001

Finite size effects and 2-string deviations in the spin-1 XXZ chains

Árpád Hegedűs

Research Institute for Particle and Nuclear Physics, Hungarian Academy of Sciences, PO Box 49, H-1525 Budapest 114, Hungary

Received 25 June 2007, in final form 29 August 2007
Published 18 September 2007
Online at stacks.iop.org/JPhysA/40/12007

Abstract

In an earlier work, Suzuki (2004 *J. Phys. A: Math. Gen.* **37** 11957) proposed a set of nonlinear integral equations (NLIE) to describe the excited state spectrum of the integrable spin-1 XXZ chain in its repulsive regime. In this paper, we extend his equations for the attractive regime of the model, and calculate analytically the conformal spectrum of the spin chain. We also discuss the typical root configurations of the thermodynamic limit as well as the 2-string deviations of certain excited states of the model. Special objects appearing in the NLIE are also treated with special care.

PACS numbers: 02.30.Ik, 75.10.Jm, 75.10.Pq

1. Introduction

Recently, spin-1 chains and quantum field theories related to the 19-vertex model [2] attract much attention. The spin-1 XXZ chains deducible from the 19-vertex model are interesting because on the one hand their Hamiltonian occurs in large N_c QCD as the 1-loop anomalous dimension matrix of the single trace operators containing the self-dual components of the field strength tensor [3], and on the other hand the determination of correlation functions in these integrable higher spin chains is still an area of active research [4]. Furthermore, it is known that in the context of light-cone approach [5] the inhomogeneous 19-vertex model with alternating inhomogeneities provides an integrable lattice regularization for the $\mathcal{N} = 1$ supersymmetric sine-Gordon model [6, 7].

In this paper, we investigate the finite size effects and 2-string deviations of the integrable spin-1 XXZ chain. It is well known that in the thermodynamic limit the anti-ferromagnetic ground state of the model is composed of quasi 2-strings, namely of pairs of complex roots having imaginary parts close to $\pm\frac{\pi}{2}$. The deviations of their imaginary parts from the values $\pm\frac{\pi}{2}$ are called 2-string deviations. According to the string hypothesis these deviations should be exponentially small in N [8–10], but it turns out that these deviations are much larger; they are of order $1/N$ [11, 12]. This is because the number of 2-strings is not of order 1, but $N/2$ minus $O(1)$, such that the centers of the outermost 2-strings tend to infinity as N tends

to infinity. This is why these 2-string deviations are not negligible even in the large N limit calculations of the physical quantities. To treat correctly the technical difficulties coming from 2-string deviations one needs to use the so-called nonlinear integral equation technique (NLIE). The NLIE technique was originally introduced in [12] where with the help of this technique the finite size effects of the ground states of the spin-1/2 and spin-1 XXZ chains were studied calculating analytically their central charges and in the spin-1 case the 2-string deviations in the ground state for the first time in a unified NLIE approach. Then the NLIE technique was successfully applied for describing finite size effects in various integrable spin chains and quantum field theories [14–20].

Recently, Suzuki [1] derived a set of NLIEs (different from those of [12]) to describe the excited states of the integrable spin-1 XXZ chain in its repulsive regime (i.e. $0 < \gamma < \frac{\pi}{3}$). In this paper, we extend his results also for the attractive regime of the model (i.e. $\frac{\pi}{3} < \gamma < \frac{\pi}{2}$). With the help of our NLIEs, we determine the operator content of the conformal field theory describing the thermodynamic limit of the spin chain. Furthermore, the NLIE enables us to discuss the typical root configurations and 2-string deviations of excited states in the large N limit.

The paper is organized as follows. In section 2, some generalities concerning the Bethe ansatz solution of the models under consideration are recalled. In section 3, the classification of the Bethe roots is presented. The auxiliary functions and their most important properties are listed in section 4. The presentation of the NLIEs can be found in section 5. Section 6 contains the counting equations, and section 7 is devoted for the discussion of typical root configurations of the thermodynamic limit. Section 8 contains the quantitative analysis of 2-string deviations and in section 9 the calculation of the conformal spectrum of the spin chain is presented. Section 10 is devoted to special objects. Finally, the summary and perspectives for future work can be found in section 11.

2. The definition of the model

The integrable spin-1 XXZ chain is defined by its Hamiltonian:

$$\mathcal{H} = \sum_{i=1}^{N} \left(\sigma_i^{\perp} - \left(\sigma_i^{\perp}\right)^2 + \cos 2\gamma \left(\sigma_i^z - \left(\sigma_i^z\right)^2\right) - (2\cos\gamma - 1)\left(\sigma_i^{\perp}\sigma_i^z + \sigma_i^z\sigma_i^{\perp}\right) - 4\sin^2\gamma \left(S_i^z\right)^2\right), \tag{1}$$

where

$$\sigma_i = S_i \cdot S_{i+1} = \sigma_i^{\perp} + \sigma_i^z, \qquad \sigma_i^z = S_i^z \cdot S_{i+1}^z.$$

In the rest of the paper, we consider N to be even and we impose periodic boundary conditions on the spins $S_{N+1}^a = S_1^a$, $a \in \{x, y, z\}$.

It is well known that the above spin Hamiltonian can be obtained from the transfer matrix of the 19-vertex model [8–10]. Hereafter, we consider the 19-vertex model with alternating inhomogeneities in order to get access to the light-cone Hamiltonian of the $\mathcal{N} = 1$ supersymmetric sine-Gordon model as well.

Let $V_i \simeq \mathbb{C}^{l_i+1}$ be the irreducible $SU(2)$ representation with spin $l_i/2$ and $R_{ij}^{(l_i,l_j)}(\theta)$ be the R-matrices acting on $V_i \otimes V_j$ satisfying the Yang–Baxter equations:

$$R_{12}^{(l_1,l_2)}(\theta) R_{13}^{(l_1,l_3)}(\theta+\theta') R_{23}^{(l_2,l_3)}(\theta') = R_{23}^{(l_2,l_3)}(\theta') R_{13}^{(l_1,l_3)}(\theta+\theta') R_{12}^{(l_1,l_2)}(\theta). \tag{2}$$

These R-matrices can be obtained by fusion [21] from the well-known R-matrix of the 6-vertex model, and their explicit form can be found in [9, 10].

From these R-matrices, one can define a family of transfer matrices with alternating inhomogeneities $\lambda_i = (-1)^i\Theta$:

$$T_k(\theta,\{\lambda_i\}) = \mathrm{Tr}_a\left(R^{(k,2)}_{a1}\left(\theta-\lambda_1-\mathrm{i}\frac{\pi}{2}(1+k)\right)\cdots R^{(k,2)}_{aN}\left(\theta-\lambda_N-\mathrm{i}\frac{\pi}{2}(1+k)\right)\right). \tag{3}$$

Due to the Yang–Baxter relation (2), the transfer matrices (3) form a commutative family of operators acting on $V_H = \otimes_{i=1}^N \mathbb{C}^3$:

$$[T_k(\theta,\{\lambda_i\}), T_{k'}(\theta',\{\lambda_i\})] = 0. \tag{4}$$

Investigating only the case of alternating inhomogeneities we can write for short $T_k(\theta,\Theta) = T_k(\theta,\{(-1)^i\Theta\})$. Due to integrability and commutativity, all these transfer matrices can be diagonalized by algebraic Bethe ansatz [28]. The eigenvalues of the transfer matrices can be characterized by the solutions of the Bethe ansatz equations:

$$\frac{\Phi(\theta_j+\mathrm{i}\pi)}{\Phi(\theta_j-\mathrm{i}\pi)} = -\frac{Q(\theta_j+\mathrm{i}\pi)}{Q(\theta_j-\mathrm{i}\pi)}, \qquad j=1,\ldots,M, \tag{5}$$

where

$$\Phi(\theta) = \left(\sinh\frac{\gamma}{\pi}(\theta-\Theta)\sinh\frac{\gamma}{\pi}(\theta+\Theta)\right)^{N/2}, \tag{6}$$

$$Q(\theta) = \prod_{j=1}^{M}\sinh\frac{\gamma}{\pi}(\theta-\theta_j), \tag{7}$$

where γ is the anisotropy of the modeland M is the number of Bethe roots. We recall that $S = N - M$ is the third component of the total spin of the spin chain. The eigenvalues of the first two transfer matrices of the fusion hierarchy can be expressed by the solutions of the Bethe ansatz equations as follows:

$$T_1(\theta,\Theta) = \Phi(\theta-\mathrm{i}\pi)\frac{Q(\theta+\mathrm{i}\pi)}{Q(\theta)} + \Phi(\theta+\mathrm{i}\pi)\frac{Q(\theta-\mathrm{i}\pi)}{Q(\theta)}, \tag{8}$$

$$\begin{aligned} T_2(\theta,\Theta) = {} & \Phi\left(\theta-\mathrm{i}\frac{\pi}{2}\right)\Phi\left(\theta-\mathrm{i}\frac{3\pi}{2}\right)\frac{Q\left(\theta+\mathrm{i}\frac{3\pi}{2}\right)}{Q\left(\theta-\mathrm{i}\frac{\pi}{2}\right)} + \Phi\left(\theta+\mathrm{i}\frac{\pi}{2}\right)\Phi\left(\theta+\mathrm{i}\frac{3\pi}{2}\right)\frac{Q\left(\theta-\mathrm{i}\frac{3\pi}{2}\right)}{Q\left(\theta+\mathrm{i}\frac{\pi}{2}\right)} \\ & + \Phi\left(\theta-\mathrm{i}\frac{\pi}{2}\right)\Phi\left(\theta+\mathrm{i}\frac{\pi}{2}\right)\frac{Q\left(\theta+\mathrm{i}\frac{3\pi}{2}\right)}{Q\left(\theta-\mathrm{i}\frac{\pi}{2}\right)}\frac{Q\left(\theta-\mathrm{i}\frac{3\pi}{2}\right)}{Q\left(\theta+\mathrm{i}\frac{\pi}{2}\right)}. \end{aligned} \tag{9}$$

The spin Hamiltonian (1) is given by the logarithmic derivative of the homogeneous transfer matrix $T_2(\theta,0)$:

$$\mathcal{H} = \frac{\pi}{\gamma}\frac{\mathrm{d}}{\mathrm{d}\theta}\log T_2(\theta,0)|_{\theta=-\mathrm{i}\frac{\pi}{2}}. \tag{10}$$

On the other hand, the regularized finite volume light-cone Hamiltonian of the $\mathcal{N}=1$ supersymmetric sine-Gordon model can be expressed by the inhomogeneous transfer matrix $T_2(\theta,\Theta)$:

$$\mathrm{e}^{\mathrm{i}a(H\pm P)/2} \sim T_2\left(\pm\Theta\pm\mathrm{i}\frac{\pi}{2},\Theta\right), \tag{11}$$

where $a = L/N$ is the lattice constant, and the continuum limit is achieved by taking N to infinity along with tuning the inhomogeneity parameter as $\Theta = \ln\frac{2N}{mL}$, with m being the kink mass.

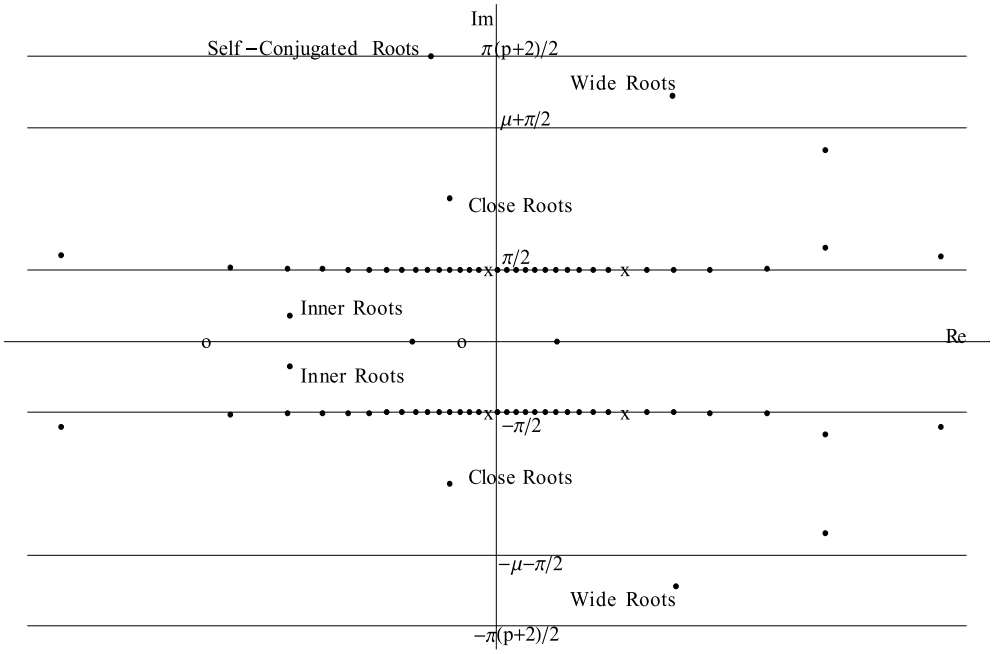

Figure 1. Classification of the Bethe roots. Crosses stand for the 2-string holes, empty circles denote the type I holes, black dots represent the Bethe roots and μ denotes $\pi\min(1, p)$.

3. Classification of the Bethe roots

First of all let us parametrize the anisotropy γ as

$$\gamma = \frac{\pi}{p+2}, \qquad 0 < p. \tag{12}$$

In this notation, the attractive $\left(\frac{\pi}{3} < \gamma < \frac{\pi}{2}\right)$ and the repulsive $\left(0 < \gamma < \frac{\pi}{3}\right)$ regimes of the model correspond to the $0 < p < 1$ and $1 < p$ regions, respectively.

All functions entering the Bethe ansatz equations (5) are periodic with respect to $\pi(p+2)$, thus on the complex plane the domain of the Bethe roots can be restricted to the strip $-\frac{\pi(p+2)}{2} < \mathrm{Im}\,\theta \leqslant \frac{\pi(p+2)}{2}$. The Bethe roots are either real or come in complex conjugated pairs, with the exception of self-conjugated roots with $\mathrm{Im}\,\theta_j = \frac{\pi(p+2)}{2}$. It is well known that the ground state of the model is formed by $N/2$ quasi 2-strings, namely the pairs of the Bethe roots with imaginary parts being close to $\pm\frac{\pi}{2}$ [8–10]. The root configurations of the excitations can be obtained from that of the ground state by adding some other new Bethe roots and removing some 2-strings. We classify the Bethe roots as follows: (see figure 1)

(1) *Inner roots*: $|\mathrm{Im}\,\theta_j| < \frac{\pi}{2}$.
(2) *Close roots*: $\frac{\pi}{2} < |\mathrm{Im}\,\theta_j| < \frac{\pi}{2} + \min(1, p)\pi$.
(3) *Wide roots*: $\frac{\pi}{2} + \min(1, p)\pi < |\mathrm{Im}\,\theta_j| < \frac{\pi(p+2)}{2}$.
(4) *Self-conjugated roots*: $|\mathrm{Im}\,\theta_j| = \frac{\pi(p+2)}{2}$.

In this classification, the quasi 2-strings can be either inner or close roots. Having derived the NLIE governing the finite size effects of the model, we will give a more precise classification of the Bethe roots.

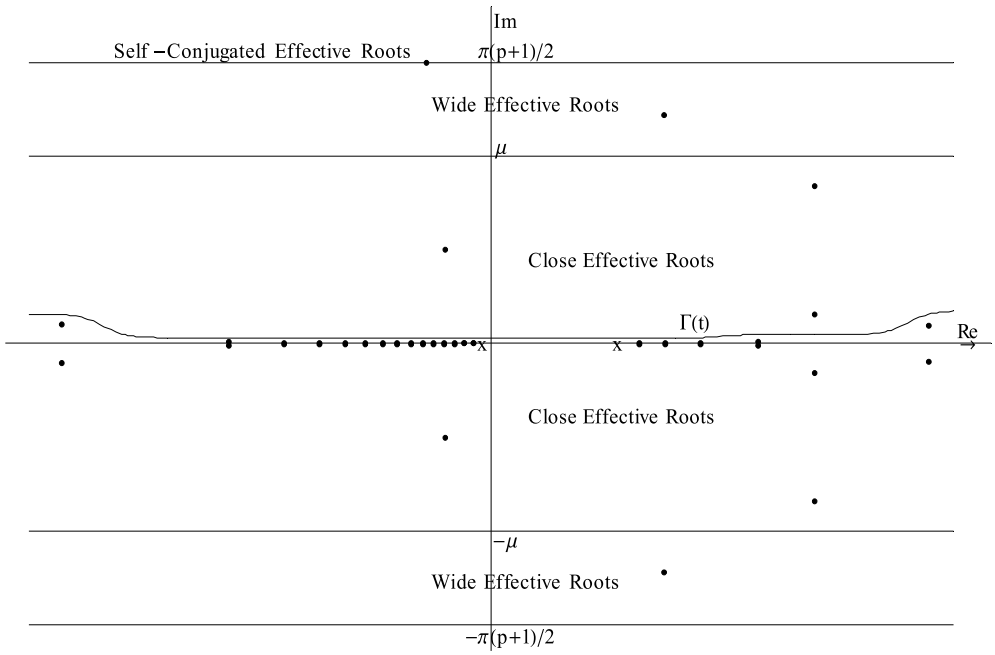

Figure 2. Classification of effective roots. Crosses stand for holes, effective roots are represented by black dots and μ denotes $\pi\min(1, p)$.

It is worth introducing the concept of *effective roots* as well. To each root θ_j with $\frac{\pi}{2} < |\mathrm{Im}\,\theta_j| \leqslant \frac{\pi(p+2)}{2}$, we associate an *effective root* $\tilde{\theta}_j$ by the following definition:

$$\tilde{\theta}_j = \theta_j - \mathrm{i}\frac{\pi}{2}\,\mathrm{sign}(\mathrm{Im}\,\theta_j). \tag{13}$$

This transformation is equivalent to the removal of the middle strip of inner roots from the fundamental domain of the original Bethe roots (see figure 2).

The classification of *effective roots* is as follows:

(1) *Close effective roots*: $0 < |\mathrm{Im}\,\tilde{\theta}_j| < \min(1, p)\pi$.
(2) *Wide effective roots*: $\min(1, p)\pi < |\mathrm{Im}\,\tilde{\theta}_j| < \frac{\pi(p+1)}{2}$.
(3) *Self-conjugated effective roots*: $|\mathrm{Im}\,\tilde{\theta}_j| = \frac{\pi(p+1)}{2}$.

The fundamental domain and the classification of effective roots are exactly the same as those of the Bethe roots in the 6-vertex model, corresponding to the bosonic degrees of freedom of the conformal field theory describing the thermodynamic limit of the spin chain.

4. Auxiliary functions and their most important properties

In this paper, we study the finite size effects of our model with the help of a set of nonlinear integral equations (NLIE). In this technique, the contribution of the $N/2$ minus $O(1)$ number of quasi 2-strings is summed up by the integral terms of the NLIE, and one has to deal with only a finite number of holes and other type of complex roots characterizing the excitation [1]. This technique is very efficient when one is interested in the spectrum of our model in the

thermodynamic limit. The first step to formulate the NLIE is the definition of proper auxiliary functions. Here we use the auxiliary functions introduced in [1, 16].

The most natural auxiliary function $a(\theta)$ is defined by

$$a(\theta) = \frac{\Phi(\theta + \mathrm{i}\pi)}{\Phi(\theta - \mathrm{i}\pi)} \frac{Q(\theta - \mathrm{i}\pi)}{Q(\theta + \mathrm{i}\pi)}, \tag{14}$$

$$1 + a(\theta) = \frac{1}{\Phi(\theta - \mathrm{i}\pi)} \frac{Q(\theta)}{Q(\theta + \mathrm{i}\pi)} T_1(\theta). \tag{15}$$

By the help of $a(\theta)$, the Bethe ansatz equations (5) can be recasted into the form

$$a(\theta_j) = -1, \qquad j = 1, \ldots, M.$$

Written in logarithmic form

$$\mathrm{i} \log a(\theta_j) = 2\pi I_j, \qquad j = 1, \ldots, M,$$

with the I_j quantum numbers being half-integers. From (15) one can see that $\mathrm{i} \log a(\theta)$ takes the value of 2π times a half-integer number also at the positions of the zeroes of $T_1(\theta)$. Thus, taking $\mathrm{i} \log a(\theta)$ on the real axis, one can interpret this function as the counting function of the real Bethe roots, because the integer part of $\mathrm{i} \frac{\log a(\theta') - \log a(\theta)}{2\pi} + 1$ provides the sum of the number of those real Bethe roots and real zeroes of $T_1(\theta)$ which lie in the interval $[\theta, \theta']$. Using this counting function, the real zeroes of $T_1(\theta)$ can be considered as holes in the distribution of the real Bethe roots, hence we will call them *type I holes* (see figure 1). The function $a(\theta)$ is important for us for the determination of the real zeroes of $T_1(\theta)$ and for the determination of wide roots in the repulsive regime.

We saw that the previous auxiliary function is the counting function of real roots but, since the ground state of the spin-1 chain is formed by 2-strings, we need to define an auxiliary function, which can be considered in the thermodynamic limit as the counting function of 2-strings. The definition of such an auxiliary function is as follows [1, 16]:

$$b(\theta) = \frac{\Phi\left(\theta - \mathrm{i}\frac{\pi}{2}\right)}{\Phi\left(\theta + \mathrm{i}\frac{\pi}{2}\right)\Phi\left(\theta + \mathrm{i}\frac{3\pi}{2}\right)} \frac{Q\left(\theta + \mathrm{i}\frac{3\pi}{2}\right)}{Q\left(\theta - \mathrm{i}\frac{3\pi}{2}\right)} T_1\left(\theta - \mathrm{i}\frac{\pi}{2}\right), \tag{16}$$

$$B(\theta) = 1 + b(\theta) = \frac{1}{\Phi\left(\theta + \mathrm{i}\frac{\pi}{2}\right)\Phi\left(\theta + \mathrm{i}\frac{3\pi}{2}\right)} \frac{Q\left(\theta + \mathrm{i}\frac{\pi}{2}\right)}{Q\left(\theta - \mathrm{i}\frac{3\pi}{2}\right)} T_2(\theta). \tag{17}$$

We also introduce the complex conjugate of $b(\theta)$ and $B(\theta)$ as auxiliary functions and denote them by $\bar{b}(\theta)$ and $\bar{B}(\theta)$, respectively.

In the thermodynamic limit, the function $\frac{1}{\mathrm{i}} \log b(\theta)$ can be considered as the counting function of 2-strings. The argument is as follows: from the definitions (16) and (17) one can see that

$$\frac{1}{\mathrm{i}} \log b\left(\theta_j - \mathrm{i}\frac{\pi}{2}\right) = 2\pi I_j, \qquad I_j \in \mathbb{Z} + \frac{1}{2}, \qquad j = 1, \ldots, M, \tag{18}$$

$$\frac{1}{\mathrm{i}} \log b(h_j) = 2\pi I_{h_j}, \qquad I_{h_j} \in \mathbb{Z} + \frac{1}{2}, \tag{19}$$

where h_j is a zero of $T_2(\theta)$. In the large N limit the 2-strings can be thought to be exact, and thus following from (18) and (19), in this limit considering the function $\frac{1}{\mathrm{i}} \log b(\theta)$ on the real axis one can recognize that the real part of $\frac{1}{\mathrm{i}} \frac{\log b(\theta') - \log b(\theta)}{2\pi} + 1$ provides the sum of the number of real zeros of $T_2(\theta)$ lying in the interval $[\theta, \theta']$ and the number of 2-strings with

$\theta < \mathrm{Re}\,\theta_j < \theta'$. In this way, the real zeroes of the transfer matrix eigenvalue $T_2(\theta)$ can be considered as holes in the distribution of 2-strings hence we will call them simply *holes*. The holes can be depicted in the plane of effective roots, so that they lie on the real axis (see figure 2).

For the closure of the NLIE, we need to define a TBA type of auxiliary function as well:

$$y(\theta) = \frac{T_2(\theta)}{\Phi\big(\theta - \mathrm{i}\frac{3\pi}{2}\big)\Phi\big(\theta + \mathrm{i}\frac{3\pi}{2}\big)}, \qquad Y(\theta) = 1 + y(\theta). \tag{20}$$

An additional auxiliary function has to be defined for the determination of wide roots in the attractive regime. Its definition is as follows:

$$h(\theta) = (-1)^M \frac{\Phi\big(\theta - \mathrm{i}\frac{\pi}{2} - \mathrm{i}p\pi\big)}{\Phi\big(\theta - \mathrm{i}\frac{\pi}{2}\big)} \frac{Q\big(\theta - \mathrm{i}\frac{3\pi}{2}\big)}{Q\big(\theta + \mathrm{i}\frac{\pi}{2} - \mathrm{i}p\pi\big)} \frac{T_1\big(\theta - \mathrm{i}\frac{\pi}{2} - \mathrm{i}p\pi\big)}{T_1\big(\theta - \mathrm{i}\frac{\pi}{2}\big)}. \tag{21}$$

In the context of the NLIE technique, the function $h(\theta)$ turns out to be the most convenient to determine the positions of wide roots. It gives the quantization rule

$$h\left(\theta_j - \mathrm{i}\frac{\pi}{2}\right) = -1$$

for the θ_j wide roots lying on the upper half of the complex plane.

In order to get the proper NLIE, one needs to know the analytic properties of the main building blocks (i.e. $Q(\theta), T_1(\theta), T_2(\theta)$) of the auxiliary functions (14)–(21). Based on numerical evidence these are as follows [1, 16]:

(1) The number of zeroes of $Q(\theta)$ with imaginary parts being close to $\pm\mathrm{i}\frac{\pi}{2}$ is N minus $O(1)$, and it has of order 1 number of zeroes located outside of this region.
(2) $T_1(\theta)$ is analytic and nonzero (ANZ) in the strip $\mathrm{Im}\,\theta \in [-\pi/2, \pi/2]$ apart from a finite number of zeroes located exactly on the real axis:

$$T_1\big(h_j^{(1)}\big) = 0, \qquad j = 1, \ldots, N_1. \tag{22}$$

(3) Also, $T_2(\theta)$ has only a finite number of zeroes in the strip $\mathrm{Im}\,\theta \in [-\pi/2, \pi/2]$ and they are also distributed along the real axis:

$$T_2(h_j) = 0, \qquad j = 1, \ldots, N_H. \tag{23}$$

The knowledge of the analytic properties of these building blocks enables us to determine easily the analytic properties of the auxiliary functions (14)–(21) which provide the starting point for the derivation of the NLIE [1, 16].

5. The nonlinear integral equations

In this section, we present the NLIE governing the finite size scaling of the inhomogeneous 19-vertex model with alternating inhomogeneities. Previously in [1] the NLIE has been derived for the repulsive regime ($1 < p$), and now we extend these results for the attractive regime ($0 < p < 1$) of the model as well. Apart from some technical subtleties, the derivation of the NLIE in the attractive regime is the same as in the repulsive one. Skipping the derivation of the NLIE and referring the interested reader to references [1, 16], we simply present the final form of the NLIE:

$$\begin{aligned}\log b(\theta) &= C_b + \mathrm{i}D(\theta) + \mathrm{i}g_1(\theta) + \mathrm{i}g_b(\theta) + (G *_{\Gamma} \ln B)(\theta) - (G *_{\tilde{\Gamma}} \ln \bar{B})(\theta) \\ &\quad + \lim_{\varepsilon \to 0^+} \big(K^{+\frac{\pi}{2}-\varepsilon} * \ln Y\big)(\theta), \\ \log y(\theta) &= C_y + \mathrm{i}g_y(\theta) + \big(K^{+\frac{\pi}{2}} *_{\Gamma} \ln B\big)(\theta) + \big(K^{-\frac{\pi}{2}} *_{\tilde{\Gamma}} \ln \bar{B}\big)(\theta),\end{aligned} \tag{24}$$

where 'ln' denotes the 'fundamental' logarithm function having its branch cut on the negative real axis and we introduced the notation for any function f

$$f^{\pm\eta}(\theta) = f(\theta \pm \mathrm{i}\eta).$$

Equations (24) contain three type of convolutions, one of them is the usual one containing integration along the real axis,

$$(f * g)(x) = \int_{-\infty}^{\infty} \mathrm{d}y\, f(x-y)g(y),$$

while the other two are defined by integrating on the complex plane along the integration contours $\Gamma(t)$ and $\bar{\Gamma}(t)$ $(t \in \mathbb{R})$:

$$(f *_{\Gamma} g)(x) = \int_{\Gamma} \mathrm{d}z\, f(x-z)g(z), \qquad (f *_{\bar{\Gamma}} g)(x) = \int_{\bar{\Gamma}} \mathrm{d}z\, f(x-z)g(z),$$

where the curve $\bar{\Gamma}(t)$ is the complex conjugate of $\Gamma(t)$. The continuous non-self-intersecting contour $\Gamma(t)$ has to fulfil the following properties:

(1) $\mathrm{Re}\,\Gamma(\pm\infty) = \pm\infty$,
(2) $0 \leqslant \mathrm{Im}\,\Gamma(t) < \min(1, p)\pi/2, \qquad \forall\, t \in \mathbb{R}.$
The first property means that the curve $\Gamma(t)$ goes to infinity in both directions and the second one is necessary to avoid the poles of the kernels $G(x)$ and $K(x)$. Although the form of equations (24) can describe correctly the finite size effects of the spin-1 chain with any choice of the contour $\Gamma(t)$ fulfilling the previous properties but, since we would like to treat only a few number of roots and holes characterizing the excitations, we impose a third condition on $\Gamma(t)$ to be fulfilled, namely.
(3) With the exception of a finite number of Bethe roots: $|\mathrm{Im}\,\theta_j| < \pi/2 + \mathrm{Im}\,\Gamma(\mathrm{Re}\,\theta_j)$, or equivalently, with the exception of a finite number of effective roots: $|\mathrm{Im}\,\tilde{\theta}_j| < \mathrm{Im}\,\Gamma(\mathrm{Re}\,\tilde{\theta}_j)$.

This third condition ensures that we need to treat only of order 1 number of roots and holes to characterize the excitations (see figure 2).

The kernel functions G and K of (24) read

$$G(\theta) = \int_{-\infty}^{\infty} \frac{\mathrm{d}q}{2\pi}\, \mathrm{e}^{\mathrm{i}q\theta}\, \frac{\sinh\frac{\pi(p-1)q}{2}}{2\sinh\frac{\pi pq}{2}\cosh\frac{\pi q}{2}}, \qquad K(\theta) = \frac{1}{2\pi\cosh(\theta)}. \tag{25}$$

We also introduce the odd primitives of the kernel functions (see appendix C for the choice of branch cuts of $\chi_K(\theta)$),

$$\chi(\theta) = 2\pi\int_0^{\theta} \mathrm{d}x\, G(x), \qquad \chi_K(\theta) = 2\pi\int_0^{\theta} \mathrm{d}x\, K(x), \tag{26}$$

that are important in writing the source terms containing information on the excitations:

$$g_b(\theta) = \sum_{j=1}^{N_H} \chi(\theta - h_j) + \sum_{j=1}^{N_V^S} (\chi(\theta - v_j) + \chi(\theta - \bar{v}_j)) - \sum_{j=1}^{N_S} (\chi(\theta - s_j) + \chi(\theta - \bar{s}_j))$$
$$- \sum_{j=1}^{M_C} \chi(\theta - c_j) - \sum_{j=1}^{M_W} \chi_{II}(\theta - w_j) - \sum_{j=1}^{M_{sc}} \chi_{II}\big(\theta - w_{sc}^{(j)}\big), \tag{27}$$

$$g_1(\theta) = \sum_{j=1}^{N_1} \chi_K\big(\theta - h_j^{(1)}\big), \tag{28}$$

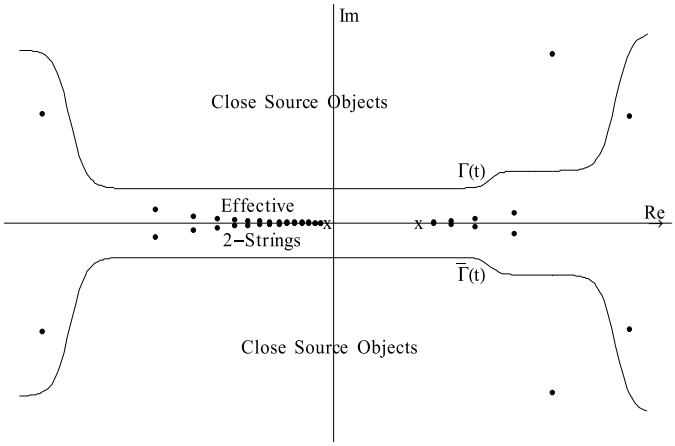

Figure 3. Zoom of figure 2 near the real axis.

$$g_y(\theta) = \lim_{\eta\to 0^+} \tilde{g}_y\left(\theta + \mathrm{i}\frac{\pi}{2} - \mathrm{i}\eta\right),$$

$$\tilde{g}_y(\theta) = \sum_{j=1}^{N_H} \chi_K(\theta - h_j) + \sum_{j=1}^{N_V^S} (\chi_K(\theta - v_j) + \chi_K(\theta - \bar{v}_j)) - \sum_{j=1}^{M_S} (\chi_K(\theta - s_j) + \chi_K(\theta - \bar{s}_j))$$
$$- \sum_{j=1}^{M_C} \chi_K(\theta - c_j) - \sum_{j=1}^{M_W} \chi_{KII}(\theta - w_j) - \sum_{j=1}^{M_{sc}} \chi_{KII}\left(\theta - w_{sc}^{(j)}\right), \tag{29}$$

where the second determination of any function, $f_{II}(\theta)$, is defined as in [17]

$$f_{II}(\theta) = \begin{cases} f(\theta) + f(\theta - \mathrm{i}\pi\ \mathrm{sign}(\mathrm{Im}\,\theta)) & 1 < p, \\ f(\theta) - f(\theta - \mathrm{i}p\pi\ \mathrm{sign}(\mathrm{Im}\,\theta)) & 0 < p < 1. \end{cases} \tag{30}$$

The objects appearing in the source terms of (24) are as follows:

(1) *Type I holes*: $\left\{h_j^{(1)}\right\}$, $j = 1, \ldots, N_1$.
(2) *Holes*: $\{h_j\}$, $j = 1, \ldots, N_H$.
(3) *Close source objects*: $\{c_j\}$ $j = 1, \ldots, M_C$, which are *close effective roots* satisfying the condition: $\mathrm{Im}\,\Gamma(\mathrm{Re}\,c_j) < |\mathrm{Im}\,c_j| < \min(1, p)\pi$ (see figures 2 and 3).
(4) *Wide effective roots*: $\{w_j\}$, $j = 1, \ldots, M_W$.
(5) *Self-conjugated effective roots*: $\left\{w_{sc}^{(j)}\right\}$, $j = 1, \ldots, M_{sc}$.

There are also two types of special objects in the source terms of our equations. It is well known that special objects appear when along the integration contour $\Gamma(t)$ the function $B(\theta)$ crosses the cut of the logarithm function [17].

It can be shown that special objects can always be avoided by an appropriate choice of the integration contour. On the other hand, it can also be shown that for any eigenstate of the Hamiltonian the contour $\Gamma(t)$ can be chosen in such a way that the NLIE must contain at least one special object. Since we want to give a formulation of the NLIE being valid for any choice of the non-self-intersecting integration contour $\Gamma(t)$, we need to take into account the special objects as well.

In our case, the special objects $\{s_j\}$ and $\{v_j\}$ are such points of the contour $\Gamma(t)$ at which the function $\ln B(\theta)$ is exactly on the cut of the logarithm, i.e. at these points the value of $B(\theta)$ is a negative real number[1].

The difference between the two types of special objects introduced above is the sign of the derivative of the imaginary part of the function $\log b(\theta)$ taken at the values of the special objects. For the objects denoted by $\{s_j\}$ this derivative is negative, and for the objects $\{v_j\}$ the derivative is positive. In the rest of the paper, we will call the objects $\{s_j\}$ *ordinary special objects* and we will call the objects $\{v_j\}$ *virtual special objects*. These special objects get the attribute 'virtual', because as we will see later in many cases one can get rid of them by an appropriate choice of the integration contour $\Gamma(t)$.

The formulation of the aforementioned conditions in the language of the function $b(\theta)$ reads

$$\operatorname{Im}\log b(s_j) = 2\pi I_{s_j}, \quad |b(s_j)| > 1, \quad (\operatorname{Im}\log b)'(s_j) < 0, \quad j = 1, \dots, N_S, \tag{31}$$

$$\operatorname{Im}\log b(v_j) = 2\pi I_{v_j}, \quad |b(v_j)| > 1, \quad (\operatorname{Im}\log b)'(v_j) > 0, \quad j = 1, \dots, N_V^S. \tag{32}$$

To provide better understanding of these special objects, we demonstrate that at special choices of the integration contour $\Gamma(t)$ the previous two types of special objects correspond to either holes or to the upper parts of the effective root counterparts of the quasi 2-strings. For the sake of simplicity, hereafter we will call the close effective roots coming from quasi 2-strings, *effective 2-strings*. When the deviations of all the quasi 2-strings are less than $\mathrm{i}\min(1, p)\frac{\pi}{2}$, the integration contour $\Gamma(t)$ can be deformed infinitesimally close to the upper parts of the effective 2-strings and the holes.

Let us single out the j_0th 2-string with a positive 2-string deviation[2]:

$$\theta_{j_0}^{\pm} = x_{j_0} \pm \mathrm{i}\left(\frac{\pi}{2} + \delta_{j_0}\right), \qquad x_{j_0}, \delta_{j_0} \in \mathbb{R}, \quad 0 < \delta_{j_0} \ll 1.$$

Then the corresponding effective 2-string takes the form: $x_0^{\pm} = x_{j_0} \pm \mathrm{i}\delta_{j_0}$. In the following, let x_0 be the position of the upper part of the effective 2-string $\left(x_0^{+}\right)$ or a hole. In this case, x_0 fulfils the quantization condition as follows:

$$\log b(x_0) = 2\pi I_0 \mathrm{i}, \qquad I_0 \in \mathbb{Z} + 1/2. \tag{33}$$

Let us assume that the integration contour $\Gamma(t)$ runs infinitesimally close to x_0, and around this point behaves like $\Gamma(t) \simeq x_0 + \mathrm{i}\eta$, with η being an infinitesimal real parameter. Then, a Taylor expansion around x_0 yields

$$\operatorname{Im}\log b(x_0 + \mathrm{i}\eta) = 2\pi I_0 + \eta(\operatorname{Re}\log b)'(x_0) + O(\eta^2), \tag{34}$$

$$\operatorname{Re}\log b(x_0 + \mathrm{i}\eta) = -\eta(\operatorname{Im}\log b)'(x_0) + O(\eta^2). \tag{35}$$

Thus, in $\eta \to 0$ limit, the $\bar{x} = x_0 + \mathrm{i}\eta$ point of the contour $\Gamma(t)$ can correspond to a special type of object (i.e. $1 + b(\bar{x})$ is a real negative number) in two cases:

(1) $0 < \eta$ and $(\operatorname{Im}\log b)'(\bar{x}) < 0$,
(2) $\eta < 0$ and $(\operatorname{Im}\log b)'(\bar{x}) > 0$.

In the first case, $\bar{x}$ is an ordinary special object satisfying (31), and in the second case $\bar{x}$ corresponds to a virtual special object defined by (32).

To summarize from the previous simple argument, it can be seen that the ordinary special objects may appear when the integration contour runs above the positions of the upper parts of

[1] The sets $\{\bar{s}_j\}$ and $\{\bar{v}_j\}$ denote the complex conjugates of the sets $\{s_j\}$ and $\{v_j\}$, respectively.
[2] Only 2-strings with positive 2-string deviations can appear in the effective plane and so in our equations.

effective 2-strings or holes, and the virtual special objects may show up when the contour $\Gamma(t)$ runs under the upper parts of the effective 2-strings. The ordinary special objects correspond to the special objects introduced in the 6-vertex model in [17].

At this point, we should mention that the best choice for the integration contour when it runs above all the upper parts of the effective 2-strings and under the upper parts of the other close effective roots, but there may be some cases (mostly in the inhomogeneous case) when due to large deviations of some quasi 2-strings, the effective 2-strings cannot be distinguished uniquely from other close effective roots, thus the differentiation between effective 2-strings and other close effective roots depends on our choice.

According to our choice, the integration contour $\Gamma(t)$ separates the effective 2-strings from those close effective roots which show up in our NLIE as close source objects. This definition is arbitrary and depends on the actual choice of the curve $\Gamma(t)$, but the NLIE (24) treats this problem consistently, and the final physical result, the energy is completely independent of the choice of this separating curve.

The driving term bulk contribution in the equation for $\ln b(\theta)$ reads

$$D(\theta) = N \arctan \frac{\sinh \theta}{\cosh \Theta}.$$

The values of the constants of the NLIE (24) are as follows:

$$C_b = \mathrm{i}\pi\delta_b, \qquad \delta_b \in \{0, 1\},$$
$$\delta_b = \frac{N}{2} + \frac{N_1}{2} - M_{sc} + S + n_- \bmod 2, \qquad n_- = \left[\frac{2S}{p+2}\right] - \left[\frac{S}{p+2}\right]$$

and

$$C_y = \mathrm{i}\pi S + \mathrm{i}\pi\Theta(p-1)(M_W + M_{sc}),$$

where $[\cdots]$ stands for the integer part and $\Theta(x)$ denotes the Heaviside function. In addition to (24), we need two other equations for the determination of type I holes and effective wide and self-conjugated roots. For the determination of type I holes, we need to know $a(\theta)$ on the real axis:

$$-\log a(\theta) = \mathrm{i}\delta_a(\theta) + (K *_\Gamma \ln B)(\theta) - (K *_\Gamma \ln \bar{B})(\theta) - C_y, \qquad 0 \leqslant |\mathrm{Im}\,\theta| < \frac{\pi}{2}, \quad (36)$$

$$\delta_a(\theta) = \sum_{j=1}^{N_H} \chi_K(\theta - h_j) + \sum_{j=1}^{N_V^S} (\chi_K(\theta - v_j) + \chi_K(\theta - \bar{v}_j)) - \sum_{j=1}^{M_S} (\chi_K(\theta - s_j) + \chi_K(\theta - \bar{s}_j))$$
$$- \sum_{j=1}^{M_C} \chi_K(\theta - c_j) - \sum_{j=1}^{M_W} \chi_{KII}(\theta - w_j) - \sum_{j=1}^{M_{sc}} \chi_{KII}\big(\theta - w_{sc}^{(j)}\big). \quad (37)$$

The function necessary to know for the determination of wide and self-conjugated effective roots is as follows: for $\min(1, p)\pi < \mathrm{Im}\,\theta \leqslant \frac{\pi(p+1)}{2}$,

$$\log \tilde{a}(\theta) = \mathrm{i}D_{II}(\theta) + \mathrm{i}g_{1II}(\theta) + \mathrm{i}g_{bII}(\theta) + (G_{II} *_\Gamma \ln B)(\theta)$$
$$- (G_{II} *_\Gamma \ln \bar{B})(\theta) + \big(\big(K^{-\frac{\pi}{2}}\big)_{II} * \ln Y\big)(\theta), \quad (38)$$

where

$$\tilde{a}(\theta) = \begin{cases} 1/a\big(\theta + \mathrm{i}\frac{\pi}{2}\big) & 1 < p, \\ 1/h(\theta) & 0 < p < 1. \end{cases} \quad (39)$$

The source objects appearing in the NLIE are not arbitrary parameters, but they have to satisfy certain quantization conditions dictated by the analytic properties of the auxiliary functions (14)–(21). These are as follows:

- For holes

$$\frac{1}{\mathrm{i}}\log b(h_j) = 2\pi I_{h_j}, \qquad j = 1, \ldots, N_H. \tag{40}$$

- For ordinary special objects

$$\mathrm{Im}\log b(s_j) = 2\pi I_{s_j}, \quad |b(s_j)| > 1, \quad (\mathrm{Im}\log b)'(s_j) < 0, \quad j = 1, \ldots, N_S. \tag{41}$$

- For virtual special objects

$$\mathrm{Im}\log b(v_j) = 2\pi I_{v_j}, \quad |b(v_j)| > 1, \quad (\mathrm{Im}\log b)'(v_j) > 1, \quad j = 1, \ldots, N_V^S. \tag{42}$$

- For close source objects (only for the upper part of the close effective pair)

$$\frac{1}{\mathrm{i}}\log b\big(c_j^{\uparrow}\big) = 2\pi I_{c_j^{\uparrow}}, \qquad j = 1, \ldots, M_C/2. \tag{43}$$

- For wide effective roots

$$\frac{1}{\mathrm{i}}\log \tilde{a}\big(w_j^{\uparrow}\big) = 2\pi I_{w_j^{\uparrow}}, \qquad j = 1, \ldots, M_W/2. \tag{44}$$

- For self-conjugated effective roots

$$\frac{1}{\mathrm{i}}\log \tilde{a}\big(w_{sc}^{\uparrow(j)}\big) = 2\pi I_{w_{sc}^{\uparrow(j)}}, \qquad j = 1, \ldots, M_{sc}. \tag{45}$$

So far we have determined only the upper part of the complex pairs, but the other parts can be determined by simple complex conjugation.

- Finally, for type I holes

$$\frac{1}{\mathrm{i}}\log a\big(h_j^{(1)}\big) = 2\pi I_{h_j^{(1)}}, \qquad j = 1, \ldots, N_1. \tag{46}$$

All the above quantum numbers I_{α_j}'s are half integers. A state is then identified by a choice of the quantum numbers $\big(I_{h_j}, I_{c_j}, \ldots\big)$. We also mention that the NLIE itself can impose constraints on the allowed values of some of these quantum numbers. To get the finite size effects of the spin chain, one needs to solve (24) supplemented by the quantization conditions (36)–(46) for the two unknown functions $b(\Gamma(t))$ and $y(x)$. Equations (36)–(46) also express the fact that the knowledge of $b(\theta)$ on a single curve $\Gamma(t)$ and $y(x)$ on the real axis is enough to be able to express all the auxiliary functions on the whole complex plane and to determine all the roots of the Bethe ansatz equations (5).

Having the solution of the NLIE, the corresponding energy eigenvalue of the spin chain can be expressed by it:

$$\begin{aligned} E = \frac{2\pi^2}{\gamma}\Bigg\{ &\sum_{j=1}^{N_H} K(h_j) + \sum_{j=1}^{N_V^S}\big(K(v_j) + K(\bar{v}_j)\big) - \sum_{j=1}^{N_S}\big(K(s_j) + K(\bar{s}_j)\big) - \sum_{j=1}^{M_C} K(c_j) \\ &- \sum_{j=1}^{M_W} K_{II}(w_j) - \sum_{j=1}^{M_{sc}} K_{II}\big(w_{sc}^{(j)}\big) + \frac{\mathrm{i}}{2\pi}\int_{\Gamma} \mathrm{d}\theta\, K'(\theta)\ln B(\theta) \\ &- \frac{\mathrm{i}}{2\pi}\int_{\bar{\Gamma}} \mathrm{d}\theta\, K'(\theta)\ln \bar{B}(\theta)\Bigg\}. \end{aligned} \tag{47}$$

6. Counting equations

The counting equations are certain sum rules which give the number of holes in terms of the numbers of different types of other source objects. These equations play an important role in the determination of the constant terms of the NLIE, and in the conformal analysis of the spin chain. In our spin-1 chain there are two important counting equations: one expresses the number of holes, the other one expresses the number of type I holes by the numbers of other source objects.

Starting from the counting function $\mathrm{i}\log a(\theta)$ and applying the argument of Destri and de Vega [17], one gets the counting equation for type I holes:

$$N_1 - 2N_R^S = S + M_1 + M_{sc} - M_R - 2n_-, \tag{48}$$

where M_1 denotes the sum of effective roots with the property $\frac{\pi}{2} < |\mathrm{Im}\,\tilde{\theta}_j| < \frac{\pi(p+1)}{2}$, M_R stands for the number of the real Bethe roots and N_R^S means the number of the *real special objects*. The real special objects can be either real Bethe roots or type I holes. They are called specials because at the positions of the real specials the counting function of the real Bethe roots is no more monotonically increasing, i.e. $\mathrm{i}\frac{\mathrm{d}}{\mathrm{d}x}\log a(x) < 0$.

There is also a parity constraint for the number of type I holes, namely N_1 *must be even*. The proof of this statement is related to the derivation of the second counting equation.

From the definition (16) of $b(\theta)$, it can be shown that the difference $\frac{1}{\mathrm{i}}(\log b(\infty) - \log b(-\infty))$ must be equal to 2π times an integer. Calculating this difference from equations (24), one gets that $\frac{1}{\mathrm{i}}(\log b(\infty) - \log b(-\infty)) = N_1\pi + 2\pi \times (\text{integer}) + 2\pi\big(N_H + 2N_V^S - 2N_S - M_C - 2S - 2\Theta(p-1)(M_W + M_{sc}) + 2N_+\big)\big/p$. Matching the two conditions for any values of p is possible only if N_1 is even and the expression divided by p in the last formula is equal to zero. This leads to the second counting equation:

$$N_H + 2N_V^S - 2N_S = M_C + 2S + 2\Theta(p-1)(M_W + M_{sc}) - 2N_+, \tag{49}$$

where $N_+ = \left[\frac{3S}{p+2}\right] - \left[\frac{S}{p+2}\right]$. In case of the absence of virtual special objects, the form of this counting equation is very similar to the one of the 6-vertex model [17].

7. Excitations in the large N limit

In this section, using our NLIE (24) we discuss qualitatively the typical Bethe root configurations of the spin chain (homogeneous case) in the $N \to \infty$ limit. In this limit, the 2-string deviations are small hence the integration contour $\Gamma(t)$ can go above the positions of all the effective 2-strings. Moreover, the counting function $\frac{1}{\mathrm{i}}\log b(\theta)$ is dominated by the bulk source function $D(\theta)$ as far as $-\ln N \lesssim \mathrm{Re}\,\theta \lesssim \ln N$. In this intermediate regime, $\ln B(\theta)$ is exponentially small in N, hence the integral terms containing $\ln B(\theta)$ can be dropped. The integrals containing $\ln Y(\theta)$ cannot be dropped, but their contribution is of order 1, so their contribution is only next to leading order in the large N limit. Their contribution is relevant for the determination of 2-string deviations, but irrelevant for the discussion of the qualitative root positions of the large N limit. Hereafter, we need to discuss separately the attractive and repulsive regimes of the model, because the typical root configurations other than quasi 2-strings are completely different.

7.1. Repulsive regime $1 < p$

According to (43), the positions of close source objects are to be determined from the function $\frac{1}{\mathrm{i}}\log b(\theta)$. The quantization condition (43) also tells us that the imaginary part of $\frac{1}{\mathrm{i}}\log b(\theta)$

at the positions of close source objects must be equal to zero. However the driving term $D(\theta)$ has a large imaginary part in the large N limit, which can be compensated only if the relative positions of close source objects tend to certain singularities of the source function $g_b(\theta)$. The singularities of $g_b(\theta)$ come from the function $\chi(\theta)$ which has poles at $\pm i\pi$.

Hence the cancellation of the contribution (of order N) to the imaginary part of $\frac{1}{i}\log b(\theta)$ dictates that the relative positions of close source objects must tend to $i\pi$. Consequently, in the large N limit, close source objects form pairs with a difference π in their imaginary parts:

$$c^+ = c_0 + i\left(\frac{\pi}{2} + \mu\right), \qquad c^- = c_0 - i\left(\frac{\pi}{2} - \mu\right), \qquad c_0, \mu \in \mathbb{R}, \quad 0 < \mu < \frac{\pi}{2}.$$

On the other hand, it is known that the close source objects appear in complex conjugated pairs, thus they must fall either into 2-string configurations on the effective plane ($\mu = 0$), $c^{\uparrow\downarrow} = c_0 \pm i\frac{\pi}{2}$, or into *effective quartets* with $c^{\pm\uparrow\downarrow} = c_0 \pm i\left(\frac{\pi}{2} \mp \mu\right)$, just like in the spin-1/2 XXZ chain [27].

However, our NLIE does not give any constraint on the imaginary parts of the wide roots, because there is no bulk driving term in (38). This is because $D_{II}(\theta) = 0$ in the repulsive regime. Transforming back the effective roots to the language of original Bethe roots, one gets that in the large N limit of the spin chain the possible root configurations are as follows:

(1) *Real roots*: $\mathrm{Im}\,\theta_j = 0$.
(2) *Inner roots*: $0 < |\mathrm{Im}\,\theta_j| < \frac{\pi}{2}$.
(3) *Quasi 2-strings*: $\mathrm{Im}\,\theta_j \simeq \pm\frac{\pi}{2}$.
(4) *Close roots with*: $\mathrm{Im}\,\theta_j \simeq \pm\pi$.
(5) *Close quartets with*: $\theta^{\pm\uparrow\downarrow} = \theta_0 \pm i(\pi \mp \mu)$, $0 < \mu < \frac{\pi}{2}$, $\theta_0 \in \mathbb{R}$.
(6) *Wide roots* with arbitrary imaginary parts.
(7) *Self-conjugated roots* with: $\mathrm{Im}\,\theta_j = \frac{\pi(p+2)}{2}$.

This means that in the large N limit, contrary to the prediction of the string hypothesis [8–10], in the spectrum of Bethe roots at best only 1-, 2- and 3-strings and anti-strings accompanied by quartets, wide and inner roots without constrained imaginary parts can be seen. In this regime, there are no constraints on the positions of wide and inner roots, because of the absence of driving bulk source terms in (36) and (38).

7.2. *Attractive regime* $0 < p < 1$

Contrary to the repulsive regime in the attractive case, the bulk driving term $D_{II}(\theta)$ of $\log\tilde{a}(\theta)$ is no longer zero imposing further constraint on the imaginary parts of wide roots as well. Analyzing the NLIE and following the argumentation of [17], the effective roots fall into the configurations as follows:

(1) *Arrays of the first kind* are effective root configurations containing close source objects as well. These type of arrays consist of effective roots of the form

$$\tilde{\theta}_k^{(1)\pm} = \theta \pm i(\mu - kp\pi), \qquad \tilde{\theta}_k^{(2)\pm} = \theta \pm i(\pi - \mu - (k-1)p\pi), \quad k = 0, \ldots, \left[\frac{1}{2p}\right],$$

with θ and $0 < \mu$ being real parameters. At certain special values of μ these arrays degenerate. There are two degenerate cases: *odd degenerate arrays* which contain a self-conjugated effective root at

$$\tilde{\theta}_{sc} = \theta + i\frac{\pi(p+1)}{2}, \qquad \theta \in \mathbb{R}$$

and accompanying complex pairs at

$$\tilde{\theta}_k = \theta \pm \mathrm{i}\frac{\pi(1-(2k+1)p)}{2}, \qquad k = 0, \ldots, \left[\frac{1}{2p}\right],$$

and *even degenerate ones*, which contain complex pairs of effective roots at the positions

$$\tilde{\theta}_k = \theta \pm \mathrm{i}\frac{\pi(1-2kp)}{2}, \qquad k = 0, \ldots, \left[\frac{1}{2p}\right].$$

These degenerate arrays contain exactly one pair of close source objects.

(2) *Arrays of the second kind* contain only wide and self-conjugated effective roots. The *odd ones* contain a self-conjugated effective root

$$\tilde{\theta}_{sc} = \theta + \mathrm{i}\frac{\pi(p+1)}{2}, \qquad \theta \in \mathbb{R}$$

and wide effective pairs at

$$\tilde{\theta}_k = \theta \pm \mathrm{i}\frac{\pi(1-(2k+1)p)}{2}, \qquad k = 0, \ldots, s, \quad 0 \leqslant s \leqslant \left[\frac{1}{2p}\right] - 1,$$

while the *even ones* contain only wide effective pairs

$$\tilde{\theta}_k = \theta \pm \mathrm{i}\frac{\pi(1-2kp)}{2}, \qquad k = 0, \ldots, s, \quad 0 \leqslant s \leqslant \left[\frac{1}{2p}\right] - 1.$$

The deviations of the imaginary parts of the previous effective root configurations from the formulae listed above are exponentially small in N.

Transforming back the effective roots into original Bethe roots, we get the following possible Bethe root configurations in the attractive regime of the model:

(1) *Real roots*: $\operatorname{Im}\theta_j = 0$.
(2) *Inner roots*: $0 < |\operatorname{Im}\theta_j| < \frac{\pi}{2}$.
(3) *Quasi 2-strings*: $\operatorname{Im}\theta_j \simeq \pm\frac{\pi}{2}$.
(4) *Arrays of the first kind* with Bethe roots at positions

$$\left.\begin{aligned} \theta_k{}^{(1)\pm} &= \theta \pm \mathrm{i}\left(\tfrac{\pi}{2} + \mu - kp\pi\right) \\ \theta_k{}^{(2)\pm} &= \theta \pm \mathrm{i}\left(\tfrac{3\pi}{2} - \mu - (k-1)p\pi\right) \end{aligned}\right\} \qquad k = 0, \ldots, \left[\frac{1}{2p}\right].$$

(5) *Odd degenerate arrays of the first kind*:

$$\theta_{sc} = \theta + \mathrm{i}\frac{\pi(p+2)}{2}, \qquad \theta_k = \theta \pm \mathrm{i}\frac{\pi(2-(2k+1)p)}{2}, \qquad k = 0, \ldots, \left[\frac{1}{2p}\right].$$

(6) *Even degenerate arrays of the first kind:*

$$\theta_k = \theta \pm \mathrm{i}\frac{\pi(2-2kp)}{2}, \qquad k = 0, \ldots, \left[\frac{1}{2p}\right].$$

(7) *Odd arrays of the second kind*:

$$\theta_{sc} = \theta + \mathrm{i}\frac{\pi(p+2)}{2}, \qquad \theta_k = \theta \pm \mathrm{i}\frac{\pi(2-(2k+1)p)}{2}, \qquad k = 0, \ldots, s,$$
$$0 \leqslant s \leqslant \left[\frac{1}{2p}\right] - 1.$$

(8) *Even arrays of the second kind:*

$$\theta_k = \theta \pm \mathrm{i}\frac{\pi(2-2kp)}{2}, \qquad k = 0, \ldots, s, \quad 0 \leqslant s \leqslant \left[\frac{1}{2p}\right] - 1.$$

Finally, we mention that the NLIE does not contain the inner roots as source objects, thus it does not impose any constraint on the positions of this type of Bethe roots. Knowing the solution of the NLIE, their positions can be determined from the counting function $\mathrm{i}\log a(\theta)$ of (36) by imposing the quantization condition

$$\mathrm{i}\log a\big(\theta_j^{(I)}\big) = 2\pi I_j^{(I)}, \qquad I_j^{(I)} \in \mathbb{Z} + \tfrac{1}{2}, \tag{50}$$

where the positions of inner roots are denoted by $\theta_j^{(I)}$.

8. 2-String deviations

In this section, we discuss the 2-string deviations for the ground state and for some simple excited states of the repulsive regime. The method of the calculation of 2-string deviations relies on the NLIE technique, and can be extended easily in principle for all excited states of the model.

Previously, the leading large N corrections of the 2-string deviations of the ground state of the spin-1 XXZ chain were calculated analytically in [11, 12]. Now we extend these calculations for excited states as well. Let us introduce the counting function

$$Z_b(\theta) = \frac{1}{\mathrm{i}N}\log b(\theta), \tag{51}$$

and write the quasi 2-strings as $\theta_j = x_j \pm \mathrm{i}\big(\frac{\pi}{2} + \delta_j\big)$, where x_js are the string centers and δ_js are the 2-string deviations in the imaginary direction. Then following from the definition (16) and (16) of $b(\theta)$, the quantization conditions hold as follows:

$$Z_b(x_j + \mathrm{i}\delta_j) = \frac{2\pi I_j}{N}. \tag{52}$$

Let us introduce the functions

$$\mathcal{K}(\theta) = \lim_{\varepsilon\to 0^+}\big(K^{+\frac{\pi}{2}-\varepsilon} * \ln Y\big)(\theta), \tag{53}$$

$$\mathcal{K}_b(\theta) = \frac{1}{\mathrm{i}}(G *_{\Gamma} \ln B)(\theta) - \frac{1}{\mathrm{i}}(G *_{\bar{\Gamma}} \ln \bar{B})(\theta). \tag{54}$$

Then using (24)–(30), $Z_b(\theta)$ can be written as

$$Z_b(\theta) = Z_0(\theta) + \frac{1}{\mathrm{i}N}\mathrm{Re}\,\mathcal{K}(\theta), \tag{55}$$

where

$$Z_0(\theta) = \arctan\sinh\theta + \frac{\pi\delta_b + g_1(\theta) + g_b(\theta) + \mathcal{K}_b(\theta) + \mathrm{Im}\,\mathcal{K}(\theta)}{N}. \tag{56}$$

It is important to remark that $Z_0(\theta)$ is always real on the real axis. Analyzing the formulae (55) and (56), one can recognize that in the large N limit the driving contribution for $Z_b(\theta)$ is in $Z_0(\theta)$, which is real along the real axis and the imaginary contribution coming from the term $\frac{1}{\mathrm{i}N}\mathrm{Re}\,\mathcal{K}(\theta)$ is only of order $1/N$ giving only small correction to $Z_0(\theta)$. From now on we assume that the 2-string deviations are small ($|\delta_j| \ll 1$), thus we can Taylor expand (52) around the 2-string centers:

$$\frac{2\pi I_j}{N} = Z_0(x_j) + \mathrm{i}\delta_j Z_0'(x_j) + \frac{1}{\mathrm{i}N}\mathrm{Re}\,\mathcal{K}(x_j) + \frac{\delta_j}{N}(\mathrm{Re}\,\mathcal{K})'(x_j) + O(\delta^2). \tag{57}$$

Assuming that δ_js are of order $1/N$ and requiring the equality up to this order one gets

$$\frac{2\pi I_j}{N} = Z_0(x_j), \tag{58}$$

$$\delta_j = \frac{1}{N}\frac{\mathrm{Re}\,\mathcal{K}(x_j)}{Z_0'(x_j)}. \tag{59}$$

The last formula (59) provides the analytical formula for the 2-string deviations. As it can be seen from (58) the function $Z_0(\theta)$ yields the quantization rules for the 2-string centers, thus it can be considered as the counting function of the 2-string centers. It follows that the function $Z_0'(\theta)$ is the density function of the 2-string centers, and so the 2-string deviations are inversely proportional to N times the 2-string density just as it was experienced in the case of the ground state in [11], hence our approximation is really valid as far as the density is not too small (in the middle of the distribution).

To get concrete formulae for the 2-string deviations of certain excited states, one has to solve (24) in the large N limit. Then the contribution of the function $\mathcal{K}_b(\theta)$ is negligible since it tends to zero exponentially in N. On the other hand, in the large N limit the contribution of $\mathcal{K}(\theta)$ is of order 1 providing 2-string deviations.

Let us discuss a few examples.

8.1. Ground state

As it is well known that the ground state is formed by only 2-strings and using a $\Gamma(t)$ contour with an appropriately large imaginary part there are no source terms present in the NLIE (24). Analyzing the NLIE (24), in the large N limit it turns out that $y(\theta) = 1$ and $\mathcal{K}(\theta) = \frac{1}{2}\ln 2$. Substituting these results into the formulae (56), (58) and (59), one gets the well-known formula of [11]:

$$\delta_j = \frac{\ln 2}{2N}\cosh x_j. \tag{60}$$

From this formula, one can see that the 2-string deviations can be considered to be small as long as $|x_j| \lesssim \ln N$.

8.2. 2-Hole states in the repulsive regime

From (49) one can see that the holes can appear only in pairs thus the excitations with smallest energies contain two holes. According to (48) and (49), the two holes can be accompanied by a pair of close source objects or by a single self-conjugated root and for these configurations the number of type I holes is zero ($N_1 = 0$). Let h_1 and h_2 the positions of the holes and assume that $h_1 < h_2$. Then from the large N analysis of the NLIE, one gets for all the possible configurations containing two holes that

$$y(\theta) = \tanh\left(\frac{\theta - h_1}{2}\right)\tanh\left(\frac{\theta - h_2}{2}\right).$$

Then the evaluation of $\mathcal{K}(\theta)$ [6] yields

$$\mathcal{K}(\theta) = \mathrm{i}\pi\left\{Q_1\left(\theta - \frac{h_1 + h_2}{2}\right) - Q_2(\theta - h_1) - Q_2(\theta - h_2)\right\}, \tag{61}$$

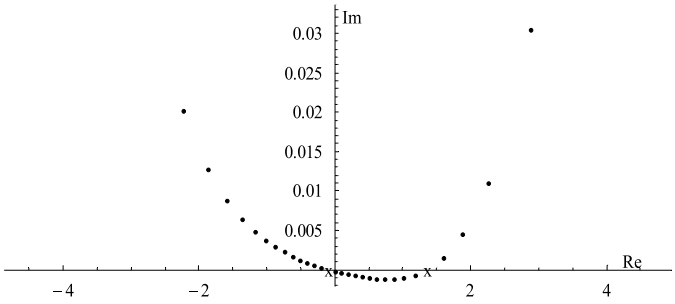

Figure 4. Deviations of the upper parts of 2-strings in a pure 2-hole state ($S = 1$) at $p = 2$, $N = 64$ with the hole quantum numbers $I_{h_1} = -1/2$ and $I_{h_2} = 12 + 1/2$.

where

$$Q_1(\theta) = -\frac{1}{2\pi}\arctan\sinh(\theta) - \frac{\mathrm{i}}{2\pi}\ln\cosh(\theta), \tag{62}$$

$$Q_2(\theta) = -\frac{\chi_2(\theta)}{2\pi} - \frac{\mathrm{i}}{2\pi}\ln\cosh\left(\frac{\theta}{2}\right), \tag{63}$$

and $\chi_2(\theta)$ denotes $\chi(\theta)$ of (26) calculated at $p = 2$. Knowing $\mathcal{K}(\theta)$ and the actual root configuration accompanying the two holes, it is easy to calculate $Z_0(\theta)$ in the large N limit. Here we do not implement this calculation but rather we concentrate on the calculation of the numerator of (59), because the sign of the numerator yields the sign of the 2-string deviations. Taking the real part of (61) along the real axis one gets

$$\mathrm{Re}\,\mathcal{K}(\theta) = \frac{1}{2}\ln\cosh\left(\theta - \frac{h_1+h_2}{2}\right) - \frac{1}{2}\ln\cosh\left(\frac{\theta-h_1}{2}\right) - \frac{1}{2}\ln\cosh\left(\frac{\theta-h_2}{2}\right). \tag{64}$$

Analyzing (64) together with (59), it turns out that the 2-string deviations are negative between the positions of the two holes (i.e. $\delta_j < 0$, if $h_1 < x_j < h_2$), and the 2-string deviations are positive outside of this region (i.e. $\delta_j > 0$, if $h_2 < x_j$ or $x_j < h_1$).

Thus, we have shown for all the 2-hole states that the 2-string deviations change sign at the positions of holes. Relying on earlier numerical studies of [23], we assume that this statement persists for multi-hole states as well. To summarize, we can say that the 2-string deviations can be positive and negative as well, and the 2-string deviations change their signs at the positions of the holes. For a numerical example, see figure 4.

However, we should remark that our derivation and so the above statement concerning the relation between the positions of holes and the signs of 2-string deviations is valid only for the middle of the root distribution, where the roots are densely distributed (i.e. $|\mathrm{Im}\,\theta| \lesssim \ln N$). Outside of this region nothing definite can be said. For example in the presence of ordinary special roots, which are typically located at the rarely distributed edges of the root distribution, there are holes at the positions of which 2-string deviations do not change sign. This can be naively explained by (59) saying that at the positions of ordinary special roots $\left(x_j^S\right)$ the density of 2-strings is negative (i.e. $Z_0'\left(x_j^S\right) < 0$), thus not only the numerator but also the denominator of (59) changes sign at the positions of certain holes.

Just to mention an example for this case, in the inhomogeneous case there exist a numerical example where $N_S = 1$, $N_H = 2$ and the two holes induced by the single ordinary special object do not change the sign of the 2-string deviations. (See figure 5 in appendix C of [6].)

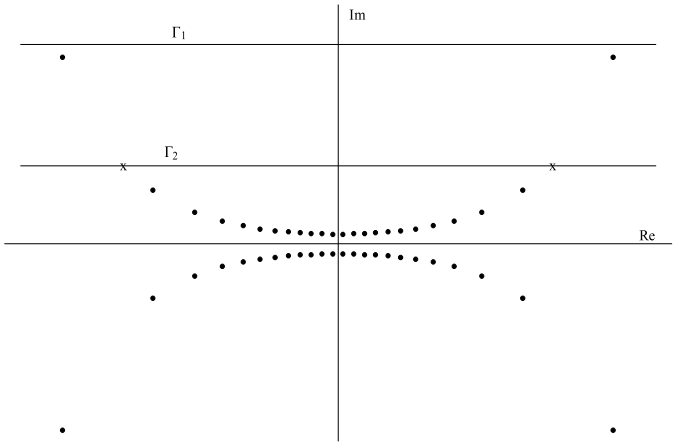

Figure 5. Effective plane and graphical demonstration of the free choice of the integration contour in case of the ground state of the model. The crosses lying on the contour Γ_2 denote the positions of the virtual special objects.

9. Conformal limit

In this section, for N even we calculate analytically the conformal spectrum of the spin chain. It is well known that the energy of the lowest lying excitations form a conformal spectrum in the large N limit, i.e. the energy levels behave as

$$E \simeq \frac{2\pi^2}{\gamma}\left(-\frac{c}{12}+\Delta^+ + \Delta^-\right)\frac{1}{N}, \tag{65}$$

where c is the central charge and $\Delta^\pm$ are the left and right conformal dimensions of the underlying conformal field theory. In this thermodynamic limit, the energy levels can be evaluated without solving the NLIE explicitly [12, 17, 22]. For the analytical calculation of the conformal spectrum, we follow the approach described in detail in [17]. The positions of the sources for $N \to \infty$ can remain finite (central objects), or they can move towards the two infinities as $\pm \ln N$ (left/right movers). We introduce the finite parts $\tilde{\theta}_j^{\pm,0}$ of their positions $\tilde{\theta}_j$ by subtracting the divergent contribution:

$$\{\tilde{\theta}_j\} \to \left\{\tilde{\theta}_j^{\pm} \pm \ln N, \tilde{\theta}_j^0\right\}.$$

We denote the number of right/left moving and central objects by $N_H^{\pm,0}$, $N_S^{\pm,0}$, $M_C^{\pm,0}, \ldots$, etc. For later convenience, we introduce the right/left moving and central spin given by

$$S^{\pm,0} = \tfrac{1}{2}\left(N_H^{\pm,0} + 2N_V^{S,\pm,0} - 2N_S^{\pm,0} - M_C^{\pm,0} - 2\Theta(p-1)\left(M_W^{\pm,0} + M_{sc}^{\pm,0}\right)\right). \tag{66}$$

According to (49), they satisfy the sum rule:

$$S^+ + S^- + S^0 = S - N_+.$$

In the thermodynamic limit, the NLIE splits into three separate equations corresponding to the three asymptotic regions. This is why for all the auxiliary functions of the NLIE (14)–(21) we define the so-called *kink functions* as

$$F_\pm(\theta) = \lim_{N\to\infty} F(\theta \pm \ln N), \qquad F \in \{\log b, \log y, \log \tilde{a}, \ldots\}. \tag{67}$$

In the large N limit, these kink functions satisfy the so-called *kink equations* and the energy and momentum can be expressed by them. Performing the above *kink limit* on our NLIE, the kink equations take the form

$$\log b_\pm(\theta) = C_b + \mathrm{i}C_{b\pm} \pm \mathrm{i}\,\mathrm{e}^{\pm\theta} + \mathrm{i}g^{(0)}_{1\pm}(\theta) + \mathrm{i}g^{(0)}_{b\pm}(\theta) + \big(G *_{\Gamma_\pm} \ln B_\pm\big)(\theta) - \big(G *_{\bar\Gamma_\pm} \ln \bar B_\pm\big)(\theta) + \big(K^{-\frac{\pi}{2}+\epsilon} * \ln Y_\pm\big)(\theta), \tag{68}$$

$$\log y_\pm\left(\theta - \mathrm{i}\frac{\pi}{2}\right) = C_y + \tilde C_{y\pm} + \mathrm{i}\tilde g^{(0)}_{y\pm}(\theta) + \big(K *_{\Gamma_\pm} \ln B_\pm\big)(\theta) - \big(K *_{\bar\Gamma_\pm} \ln \bar B_\pm\big)(\theta), \tag{69}$$

$$\log y_\pm(\theta) = \lim_{\eta\to\frac{\pi}{2}^-} \log y_\pm\left(\theta - \mathrm{i}\frac{\pi}{2} + \mathrm{i}\eta\right). \tag{70}$$

$$-\log a_\pm(\theta) = C_y + \tilde C_{y\pm} + \mathrm{i}\delta^{(0)}_{a\pm}(\theta) + \big(K *_{\Gamma_\pm} \ln B_\pm\big)(\theta) - \big(K *_{\Gamma_\pm} \ln \bar B_\pm\big)(\theta), \tag{71}$$

$$\ln \tilde a_\pm(\theta) = \mathrm{i}C^\pm_{\tilde a} + \mathrm{i}\tilde g^{(0)}_{\tilde a\pm}(\theta) + \big(G_{II} *_{\Gamma_\pm} \ln B_\pm\big)(\theta) - \big(G_{II} *_{\bar\Gamma_\pm} \ln \bar B_\pm\big)(\theta), \tag{72}$$

where the functional forms of the source functions of the kink functions (68)–(72) are the same as those of the original equations (24)–(39) with the difference that they contain only the finite part of the left- and right-moving holes and effective roots, respectively[3]. (See, for example [6].) The bulky expressions of the constant terms of equations (68)–(72) are listed in appendix B. The finite part of the right- and left-moving objects can be obtained from the kink functions by imposing quantization conditions very similar to (40)–(46).

After some manipulations [6, 12, 17, 22], it turns out that in the thermodynamic limit the energy and momentum can be expressed by a sum of dilogarithm functions with $\theta \to \pm\infty$ limiting values of the kink functions in their argument. One group of these limiting values agrees with the limiting values of the original auxiliary functions at the infinities, namely

$$b_\pm(\pm\infty) = \mathrm{e}^{\pm 3\mathrm{i}\gamma S}\, 2\cos(\gamma S), \qquad B_\pm(\pm\infty) = \mathrm{e}^{\pm 2\mathrm{i}\gamma S}\,\frac{\sin(3\gamma S)}{\sin(\gamma S)}, \tag{73}$$

$$y_\pm(\pm\infty) = \frac{\sin(3\gamma S)}{\sin(\gamma S)}, \qquad Y_\pm(\pm\infty) = 4\cos(\gamma S)^2 > 0. \tag{74}$$

The other group of limiting values of the kink functions can be determined from the kink equations (68)–(72). They read as follows:

$$b_\pm(\mp\infty) = \bar b_\pm(\mp\infty) = 0, \tag{75}$$

$$y_\pm(\mp\infty) = (-1)^{\delta^\pm_y}, \qquad \delta^\pm_y = N_+ + 2S^\pm \bmod 2. \tag{76}$$

Using the dilogarithm sum rule of appendix A, and putting everything together, one gets that the central charge is $3/2$ and the conformal weights take the form

$$\Delta^\pm = \frac{1}{16}\delta^\pm_y + \frac{1}{2}\left(\frac{Q_\pm}{R} + \frac{S}{2}R\right)^2 + \tilde N_\pm + J_\pm, \tag{77}$$

where

$$Q_\pm = S^\pm - \frac{S - N_+}{2}, \tag{78}$$

[3] Left-moving kink functions contain only the left-moving (indexed by $-$) objects, and the right-moving kink functions contain only the right-moving (indexed by +) objects in their source terms.

$$\tilde{N}_\pm = \frac{\hat{N}_+ - \delta_y^\pm}{8} + SS^\pm - \frac{3}{2}(S^\pm + N_+)S^\pm, \tag{79}$$

$$J_\pm = \mp I_{h^\pm} \mp 2I_{v^\pm} \pm 2I_{s^\pm} \pm 2I_{c^{\pm\uparrow}} \pm 2I_{w^{\pm\uparrow}} \pm I_{w_{sc}^{\pm\uparrow}} \mp I_{h^{(1)\pm}} + S^\pm \left(M_{sc}^\pm - M_{sc} + \frac{N_1}{2} - N_1^\pm + \frac{N}{2} \pm \delta_b \right) + N_{II}^\pm + \frac{1}{2}\left(M_{sc}^\pm\right)^2 \tag{80}$$

and

$$I_{h^\pm} = \sum_{j=1}^{N_H^\pm} I_{h_j^\pm}, \qquad I_{s^\pm} = \sum_{j=1}^{N_S^\pm} I_{s_j^\pm}, \qquad I_{v^\pm} = \sum_{j=1}^{N_V^{S\pm}} I_{v_j^\pm}, \qquad I_{c^{\pm\uparrow}} = \sum_{j=1}^{M_C^{\pm\uparrow}} I_{c_j^{\pm\uparrow}}, \ldots, \text{etc.}$$

Furthermore, $\hat{N}_+ = N_+ \bmod 2$ and $N_{II}^\pm$ are integers depending on the relative positions of complex effective roots and they must be determined case by case. In (77), the parameter R is the compactification radius defined by

$$R = \sqrt{\frac{p}{p+2}}. \tag{81}$$

In order that the formulae (77)–(81) describe the conformal weights of a $c = 3/2$ conformal field theory, the difference $\Delta^+ - \Delta^-$ must be independent of R. This requirement suffices, because in the conformal limit the momentum eigenvalues of the spin chain behaves as $P \sim (\Delta^+ - \Delta^-)/N$, on the other hand the operator e^{iP} is the operator which translates a state by one lattice site. Thus, due to the periodic boundary conditions after N unit translations one gets back the original state, i.e. $e^{iPN} = 1$. It follows that the eigenvalues of the momentum operator look like $P = \frac{2\pi}{N} \times$ integer hence the difference $\Delta^+ - \Delta^-$ is independent of the compactification radius R. The fact that $\Delta^+ - \Delta^-$ is independent of the compactification radius implies some constraints on the possible root configurations in the thermodynamic limit. The independence of R can be implemented in two ways:

(1) $Q_+ = Q_-$ in this case S^0 is zero.
(2) $Q_+ = -Q_-$ in this case $S^+ = S^-$.

To summarize, in the thermodynamic limit for states describing the lowest excitations[4], only such root configurations appear which carry either zero central spin ($S^0 = 0$) or their left- and right-moving spins are equal ($S^+ = S^-$).

Analyzing the formulae (77)–(81), one can see that the spin of the state can be identified with the winding number of the Gaussian part of the $c = 3/2$ CFT, and the parameters $\delta_y^\pm$ distinguish the Neveu–Schwartz and Ramond sectors. Depending on the state under consideration the sum $\tilde{N}_\pm + J_\pm$ can be either integer or half integer, but in the Ramond sector they are always integers. Furthermore, the $S^0 = 0$ and $S^+ = S^-$ conditions guarantee that $\delta_y^+ = \delta_y^-$ ensuring the correct appearance of the $1/16$ terms in the conformal weights. Moreover, further analysis of (77) shows that there is a relation between $Q_\pm$ and the winding number S, namely in the NS sector $\left(\delta_y^\pm = 0\right)$:

$$Q_\pm \in \mathbb{Z} \qquad \text{if} \quad S \in 2\mathbb{Z}, \tag{82}$$

$$Q_\pm \in \mathbb{Z} + \tfrac{1}{2} \qquad \text{if} \quad S \in 2\mathbb{Z} + 1, \tag{83}$$

[4] Roughly speaking, the 'lowest excitations' means that these excitations give only of order $1/N$ correction to the energy of the ground state. In the repulsive regime this means that $N_H^0 = 0$, because central holes would give an order 1 contribution to the energy. In case of the attractive regime also the number of the central wide effective roots is zero when we speak about the 'lowest excitations' in the large N limit.

while in the Ramond sector $\left(\delta_y^{\pm}=1\right)$:

$$Q_{\pm} \in \mathbb{Z}+\tfrac{1}{2} \qquad \text{if} \quad S \in 2\mathbb{Z}, \tag{84}$$

$$Q_{\pm} \in \mathbb{Z} \qquad \text{if} \quad S \in 2\mathbb{Z}+1. \tag{85}$$

Putting together the results of the previous analysis of the conformal weights (77)–(81), one can recognize that they can be interpreted within the framework of $c=3/2$ CFT as conformal weights appearing in the modular invariant partition function of Di Francesco *et al* [25]:

$$Z(R)=\frac{1}{|\eta|^2}\left\{(\chi_0\bar{\chi}_{1/2}+\chi_{1/2}\bar{\chi}_0)\sum_{n\in\mathbb{Z}+\frac{1}{2},m\in 2\mathbb{Z}+1}\right.$$
$$\left.+(|\chi_0|^2+|\chi_{1/2}|^2)\sum_{n\in\mathbb{Z},m\in 2\mathbb{Z}}+|\chi_{1/16}|^2\sum_{2n-m\in 2\mathbb{Z}+1}\right\}q^{\Delta^+_{n,m}}\bar{q}^{\Delta^-_{n,m}},$$

where

$$\Delta^{\pm}_{n,m}=\frac{1}{2}\left(\frac{n}{R}\pm\frac{m}{2}R\right)^2$$

are the conformal weights of the Gaussian part of the CFT, $\eta(q)$ is the Dedekind function and $q=\mathrm{e}^{2\pi\mathrm{i}\tau}$, τ being the modular parameter.

This analytical result agrees with the earlier conjecture of Alcaraz and Martins based on the numerical investigation of the Bethe ansatz equations of the spin-1 XXZ chain [24].

To close this section we remark that the results for the conformal weights (77)–(81) are analytic in the anisotropy parameter γ in the entire regime $[0,\pi/2]$, although the Bethe ansatz patterns for the excited states look qualitatively different for the repulsive and the attractive regimes. The situation is quite similar to that of the spin-1/2 chain. There, the same derivation that is successful in the repulsive regime is applicable in the attractive regime. The key to this is the large freedom in the choice of the integration contour Γ and the possibility of writing down the nonlinear integral equations that are algebraically identical to those for the ground state but using deformed contours. In this approach there are no additional 'driving terms' in the NLIEs, and the conformal charges are given in terms of dilogarithm functions with 'nonstandard' integration contours [13]. The analyticity of conformal weights in the spectral parameter indicates that this approach can probably be extended for higher spin cases too.

10. Ordinary and virtual special objects

In this section, we would like to shed more light on the appearance of virtual special objects in the NLIE, therefore we will consider the ground state as a simplest example. The ground state of the model is formed by $N/2$ quasi 2-strings with quite small deviations from $\pm\frac{\pi}{2}$ in their imaginary parts. First, let us write down the NLIE when the contour is chosen to be a straight line running above all the effective 2-strings (i.e. $\Gamma_1(t)=t+\mathrm{i}\eta_1$ with $\eta_1>\delta_j\ \forall\, j$). (See figure 5.) In this case, the NLIE takes the form of (24) with trivial source terms:

$$g_1(\theta)=g_b(\theta)=g_y(\theta)=0.$$

In this case, there are neither ordinary nor virtual special objects present.

Next, we consider another straight contour $\Gamma_2(t)$ running under exactly two effective 2-strings: (i.e. $\Gamma_2(t)=t+\mathrm{i}\eta_2$ with $\eta_2<\delta_1=\delta_{N/2}$ and $\eta_2>\delta_j$ for all other values of j). (See figure 5.) In this case, the non-bulk source terms of the NLIE are not zero anymore! Two

pairs of close source objects corresponding to the two effective 2-strings being above $\Gamma_2(t)$ appear as source terms and also two virtual special objects show up in the source term of the NLIE. In the language of the counting equation (49), the appearance of the four close source objects (i.e. $M_C = 4$) entails the appearance of two virtual special objects ensuring that we are still speaking about the ground state (i.e. $N_H = M_W = M_{sc} = S = 0$). Then compared to the previous case the source terms of (24) are modified as

$$g_b(\theta) = \chi(\theta - v_1) + \chi(\theta - \bar{v}_1) + \chi(\theta - v_{N/2}) + \chi(\theta - \bar{v}_{N/2}) - \chi(\theta - c_1) - \chi(\theta - \bar{c}_1) - \chi(\theta - c_{N/2}) - \chi(\theta - \bar{c}_{N/2}), \tag{86}$$

$$\tilde{g}_y(\theta) = \chi_K(\theta - v_1) + \chi_K(\theta - \bar{v}_1) + \chi_K(\theta - v_{N/2}) + \chi_K(\theta - \bar{v}_{N/2}) - \chi_K(\theta - c_1) - \chi_K(\theta - \bar{c}_1) - \chi_K(\theta - c_{N/2}) - \chi_K(\theta - \bar{c}_{N/2}), \tag{87}$$

and $g_1(\theta) = 0$. As for the notation v_1 and $v_{N/2}$ denotes the positions of the virtual special objects and the set $\{c_1, c_{N/2}, \bar{c}_1, \bar{c}_{N/2}\} = \{\pm x_1 \pm \mathrm{i}\delta_1\}$ denotes the set of close source objects. These source objects are subjected to quantization conditions, namely c_1, and $c_{N/2}$ satisfy a condition like (43), and v_1, and $v_{N/2}$ have to satisfy (42). The other source objects are simply complex conjugates of these ones. This was the simplest example how the virtual special objects enter the NLIE. Nevertheless, we have to note that although the two different formulations of the NLIE for the ground state are equivalent but they are not equally practical! The second formulation containing virtual special objects is not appropriate for numerical studies, because the usual large N iteration of the NLIE fails to converge, while the first formulation of the NLIE can be solved easily numerically. Certainly, when analytical calculations are considered (e.g. the calculation of conformal weights) they can be used equally well, and they give the same result. To summarize, the same state can be formulated in many ways by means of the NLIE by the modification of the contour $\Gamma(t)$. The different formulations differ from each other in the number of virtual special objects occurring in the source terms.

The ordinary special objects defined by (31) according to the counting equation (49) are generally accompanied by the appearance of two holes, just like in the 6-vertex model. Taking a glance at the NLIE (24), ordinary special objects may pop up in those regimes where the derivative of the bulk source term $D(\theta)$ becomes small. This means that in the spin chain they can appear at the edges of the root distribution (i.e. $\ln N \lesssim |\mathrm{Re}\,\theta|$). In case of alternating inhomogeneities, if the inhomogeneity parameter Θ scales as $\ln N$ as $N \to \infty$ then ordinary special objects may emerge in the middle of the root distribution or at its edges. In the inhomogeneous case, a nice numerical example for ordinary special objects can be found in appendix C of [6]. We remark that when any type of special objects show up in the form of the NLIE then its numerical solution fails to converge, thus in the presence of specials one can rely on only analytical manipulations of the NLIE.

11. Summary and perspectives

In this paper, we extended Suzuki's NLIE for the attractive regime $\left(\frac{\pi}{3} < \gamma < \frac{\pi}{2}\right)$ of the inhomogeneous 19-vertex model with alternating inhomogeneities. Then we analyzed the NLIE corresponding to the homogeneous case to describe the finite size spectrum of the integrable spin-1 XXZ chain. Using the NLIE, we determined analytically the conformal spectrum emerging in the large N limit of the spin chain. Our result agreed with the one proposed earlier by Alcaraz and Martins based on the numerical investigation of the Bethe ansatz equations [24]. By means of the NLIE, we discussed the typical Bethe root

configurations of the thermodynamic limit, and we worked out a method to determine the 2-string deviations for any eigenstate of the model. Moreover, we have shown analytically for a class of excited states that, in accordance with earlier numerical observations [23], the holes in the sea of 2-strings are the positions where the 2-string deviations change sign.

Finally, we would like to make a few comments on the possible further applications of the NLIE. First of all it is worth mentioning that recently, in the framework of the quantum inverse scattering method, a remarkable progress has been made in the calculation of form factors and correlation functions of integrable spin chains [4, 26]. The correlation functions are represented as complicated multiple integrals, and the form factors of local operators are expressed as determinants of matrices, whose matrix elements are the known analytic functions of Bethe roots of the eigenstates involved. The multiple integral representations of correlation functions are too complicated for their explicit analytical or numerical evaluation. However, as it was done in [26], one can try to calculate the correlation functions numerically by formulating them as a series of appropriate form factors. In this case, the form factors are determined by their determinant representations involving the Bethe roots of the included eigenstates.

This method requires the knowledge of the Bethe roots for many eigenstates. Nevertheless, the solution of the Bethe ansatz equations in higher spin XXZ chains is not easy for large N because of the string deviations. At this point, the NLIE can be useful since it can be numerically solved easily for large N and using the definitions of the auxiliary functions, all the positions of the Bethe roots can be extracted from the numerical solution, providing a good starting point for the numerical calculation of form factors.

Another area of applications of the NLIE is the description of finite size effects in (1+1)-dimensional integrable quantum field theories. It is known that the NLIE (24) with an appropriately tuned inhomogeneity parameter describe the finite size effects in the $\mathcal{N} = 1$ supersymmetric sine-Gordon model [6, 7]. The NLIE governing the finite size effects of the $\mathcal{N} = 1$ supersymmetric sine-Gordon model in the repulsive regime was investigated in [6], and the ground state of the model with Dirichlet boundary conditions was studied in [7]. The extension of the NLIE technique to the attractive regime, presented in this paper, enables one to investigate the attractive regime of the model as well.

Acknowledgments

This investigation was supported by the Hungarian National Science Fund OTKA (under T049495).

Appendix A

In section 9, in the calculation of the conformal weights, the following dilogarithmic sum must be calculated:

$$S_0 = 2\left\{L_+[\mathrm{e}^{3\mathrm{i}\gamma S}\,2\cos(\gamma S)] + L_+[\mathrm{e}^{-3\mathrm{i}\gamma S}\,2\cos(\gamma S)] + L_+\left[\frac{\sin(3\gamma S)}{\sin(\gamma S)}\right]\right\}, \tag{A.1}$$

where

$$L_+(x) = \frac{1}{2}\int_0^x \mathrm{d}y\left\{\frac{\ln(1+y)}{y} - \frac{\ln y}{1+y}\right\}. \tag{A.2}$$

Using the dilogarithm identity of appendix B of [6], it can be easily proven that

$$S_0 = \frac{2\pi^2}{3} + \hat{N}_+\left\{2\pi\left|\gamma S - \pi\left[\frac{\gamma S}{\pi}\right] - \frac{\pi}{2}\right| - \pi^2\right\} - \mathrm{i}\hat{N}_+\pi\ln(4\cos^2(\gamma S)), \tag{A.3}$$

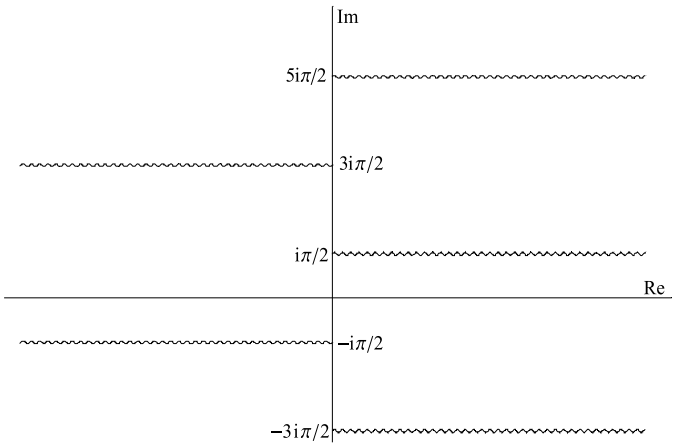

Figure 6. Locations of the branch cuts of $\chi_K(\theta)$.

where

$$\hat{N}_+ = N_+ \bmod 2, \qquad N_+ = \left[3\frac{\gamma S}{\pi}\right] - \left[\frac{\gamma S}{\pi}\right], \tag{A.4}$$

and we made the choice of $\ln(-1) = \mathrm{i}\pi$.

Appendix B

This appendix is devoted to list the constants emerging in the kink equations (68)–(72). They are as follows:

$$C_{b\pm} = \pm 2\chi_\infty(S - S^+ - N_+) \pm \pi\left(\frac{N}{2} - \left(M_{sc} - M_{sc}^\pm\right) + \frac{N_1 - N_1^\pm}{2}\right) + 2\pi K_W^\pm, \tag{B.1}$$

$$C_{y+} = \mathrm{i}\pi\left(S + M_1 - N_+ - S^+ - M_1^+\right), \tag{B.2}$$

$$C_{y-} = \mathrm{i}\pi\left(S^- + M_1^- + 2M_{sc}^- - S - M_1 + N_+ - 2M_{sc}\right), \tag{B.3}$$

$$C_{\tilde{a}\pm} = \pm 2\pi(S - S^\pm - N_+) + 2\pi N_{\tilde{a}\pm}, \tag{B.4}$$

where the integers $K_W^\pm$ and $N_{\tilde{a}\pm}$ depend on the relative positions of the wide effective roots, and they must be determined case by case.

Appendix C

In this appendix, the most important properties of the function $\chi_K(\theta)$ will be clarified. The function $\chi_K(\theta)$ is defined as the odd primitive of the kernel $2\pi K(\theta)$ and given by the formula

$$\chi_K(\theta) = \mathrm{i}\ln\frac{\sinh\left(\mathrm{i}\frac{\pi}{4} + \frac{\theta}{2}\right)}{\sinh\left(\mathrm{i}\frac{\pi}{4} - \frac{\theta}{2}\right)}, \qquad \chi_K(\theta) = -\chi_K(-\theta), \quad \forall\theta \in \mathbb{C}. \tag{C.1}$$

The branch cuts are chosen to run parallel to the real axis so that $\chi_K(\theta)$ be an odd real analytic function on the entire complex plane and continuous along the real axis. In this case, $\chi_K(\theta)$

is not periodic anymore with respect to $2\pi\mathrm{i}$. It is periodic only modulo 2π, i.e. the following identity holds:

$$\chi_K(\theta + 2\pi\mathrm{i}) = \chi_K(\theta) - 2\pi.$$

It follows that the distance between the consecutive cuts is $2\pi\mathrm{i}$ and the jump of $\chi_K(\theta)$ is equal to -2π at each branch cut crossed from down to up. The choice of branch cuts is depicted in figure 6.

References

[1] Suzuki J 2004 *J. Phys. A: Math. Gen.* **37** 11957
[2] Zamolodchikov A B and Fateev V A 1980 *Yad. Fiz.* **32** 581
[3] Ferretti G, Heise R and Zarembo K 2004 *Phys. Rev.* D **70** 074024
[4] Terras V and Maillet J M 2000 *Nucl. Phys.* B **575** 627
Kitanine N 2001 *J. Phys. A: Math. Gen.* **34** 8151
Castro-Alvaredo O A and Maillet J M 2007 *Preprint* hep-th/0702186
Idzumi M 1994 *Int. J. Mod. Phys.* A **9** 4449 (*Preprint* hep-th/9307129)
Bougourzi A H and Weston R A 1994 *Nucl. Phys.* B **417** 439
[5] Destri C and de Vega H J 1987 *Nucl. Phys.* B **290** 363
Destri C and de Vega H J 1988 *Phys. Lett.* B **201** 261
Destri C and de Vega H J 1989 *J. Phys. A: Math. Gen.* **22** 1329
[6] Hegedűs Á, Ravanini F and Suzuki J 2007 *Nucl. Phys.* B **763** 330
[7] Ahn C, Nepomechie R I and Suzuki J 2006 *Preprint* hep-th/0611136
[8] Takhtajan L A 1982 *Phys. Lett.* A **87** 497
Babujian H M 1983 *Nucl. Phys.* B **215** 317
[9] Babujian H M and Tsvelick A M 1986 *Nucl. Phys.* B **265** 24
[10] Kirillov A N and Reshetikhin N Yu 1987 *J. Phys. A: Math. Gen.* **20** 1565
[11] de Vega H J and Woynarovich F 1990 *J. Phys. A: Math. Gen.* **23** 1613
[12] Klümper A, Batchelor T M and Pearce P A 1991 *J. Phys. A: Math. Gen.* **24** 3111
Klümper A and Batchelor T M 1990 *J. Phys. A: Math. Gen.* **23** L189
[13] Klümper A, Wehner T and Zittarz J 1993 *J. Phys. A: Math. Gen.* **26** 2815
[14] Destri C and de Vega H J 1992 *Phys. Rev. Lett.* **69** 2313
Destri C and de Vega H J 1995 *Nucl. Phys.* B **438** 413
[15] Klümper A and Pearce P A 1991 *J. Stat. Phys.* **64** 13
Klümper A and Pearce P A 1992 *Physica* A **183** 304
[16] Suzuki J 1999 *J. Phys. A: Math. Gen.* **32** 2341
[17] Destri C and de Vega H J 1997 *Nucl. Phys.* B **504** 621
[18] Fioravanti D, Mariottini A, Quattrini E and Ravanini F 1997 *Phys. Lett.* B **390** 243
Feverati G, Ravanini F and Takacs G 1998 *Phys. Lett.* B **444** 442
Feverati G, Ravanini F and Takacs G 1999 *Nucl. Phys.* B **540** 543
[19] Bazhanov V V, Lukyanov S and Zamolodchikov A B 1997 *Commun. Math. Phys.* **190** 247
Bazhanov V V, Lukyanov S and Zamolodchikov A B 1997 *Nucl. Phys.* B **489** 487
[20] Dunning C 2003 *J. Phys. A: Math. Gen.* **36** 5463
Hegedüs Á 2004 *Nucl. Phys.* B **679** 545
Hegedüs Á 2005 *J. Phys. A: Math. Gen.* **38**
Hegedüs Á 2005 *Nucl. Phys.* B **732** 463
[21] Kulish P P, Reshetikhin N Yu and Sklynin E K 1981 *Lett. Math. Phys.* **5** 393
[22] Zamolodchikov Al B 1990 *Nucl. Phys.* B **342** 695
Klassen T R and Melzer E 1990 *Nucl. Phys.* B **338** 485
[23] Avdeev L V and Dörfel D 1985 *Nucl. Phys.* B **257** 253
Avdeev L V and Dörfel D 1987 *Theor. Math. Phys.* **71** 528
[24] Alcaraz F C and Martins M J 1989 *J. Phys. A: Math. Gen.* **22** 1829
[25] Di Francesco P, Saleur H and Zuber J-B 1988 *Nucl. Phys.* B **300[FS22]** 393
[26] Caux J S and Maillet J M 2005 *Phys. Rev. Lett.* **95** 077201
Caux J S, Hagemans R and Maillet J M 2005 *J. Stat. Mech.* P09003
[27] Woynarovich F 1982 *J. Phys. A: Math. Gen.* **15** 2985
[28] Faddeev L D and Takhatajan L 1979 *Usp. Mat. Nauk* **34** 5